Soft Matter

International Edition: DOI: 10.1002/anie.201412160
German Edition: DOI: 10.1002/ange.201412160

Photothermally Reprogrammable Buckling of Nanocomposite Gel Sheets**

*Adam W. Hauser, Arthur A. Evans, Jun-Hee Na, and Ryan C. Hayward**

Abstract: *Patterning deformation within the plane of thin elastic sheets represents a powerful tool for the definition of complex and stimuli-responsive 3D buckled shapes. Previous experimental methods, however, have focused on sheets that access a limited number of shapes pre-programmed into the sheet, restricting the degree of dynamic control. Here, we demonstrate on-demand reconfigurable buckling of poly(N-isopropylacrylamide-co-acrylic acid) (PNIPAM) hydrogel network films containing gold nanoparticles (AuNPs) by patterned photothermal deswelling. Predictable, easily controllable, and reversible transformations from a single flat gel sheet to numerous different three-dimensional forms are shown. Importantly, the response time is limited by poroelastic mass transport, rather than photochemical switching kinetics, enabling reconfiguration of shape on timescales of several seconds, with further increases in speed possible by reducing film thickness.*

Shape transformations driven by inhomogeneous in-plane distortion of thin elastic membranes provide powerful routes to reconfigurable 3D materials.[1–4] Thus far, most work has focused on sheets that can access only a single trajectory from flat to a particular buckled shape that is pre-programmed into the material.[5–10] The incorporation of two or more independently addressable responsive materials[11] or electrical heaters[12] provides access to several different pre-programmed shapes, but the difficulty of fabricating and controlling such patterned sheets increases rapidly with the number of orthogonally controllable elements incorporated. Alternatively, printing, erasing, and rewriting ionic species within hydrogels[13] or shape memory polymers[14] have been used to form several 3D shapes from a single material; however, these approaches involve time consuming processes for reprogramming that require physical contact with the material.

Light-addressable materials are of great interest in this respect, as they should allow for continuous reprogramming into an arbitrary number of 3D shapes defined by patterns of illumination. While Kuksenok and Balazs have modeled reconfigurable gel sheets with light-controlled swelling based on the photoisomerization of spiropyran,[15] this approach has not been experimentally realized. In addition, the reliance of photoisomerization-driven changes in swelling involves several drawbacks, most notably slow switching kinetics, incomplete reversibility, and the use of ultraviolet light.[16–20] In contrast, photothermally addressable hydrogels that rely on well-known volume–temperature transitions triggered by absorption of visible or infrared light offer switching speeds limited by mass transport, along with highly reversible and large changes in swelling.[21–26] An important limitation is that the diffusion coefficient for heat conduction is typically several orders of magnitude larger than that for poroelastic mass transport, such that heat generated locally can spread out broadly in space over the time required for the gel to reach swelling equilibrium.[15] However, for systems where the overall heat generation is small compared to dissipation into the environment, it is possible to prepare well-defined steady-state (time-invariant) spatial temperature profiles that allow for patterned swelling of thermally responsive gels.[12,25,27]

Here, to achieve arbitrary and fully reprogrammable patterns of local deformation within a single hydrogel sheet, we take advantage of heat generated due to the surface plasmon resonance (SPR) absorption of gold nanoparticles (AuNP) with a diameter of about 4 nm,[28,29] coupled with the thermal deswelling of poly(*N*-isopropylacrylamide-*co*-acrylic acid) (PNIPAM) hydrogels to drive patterned buckling of nanocomposite (NC) gel sheets, as illustrated in Figure 1 A. There are several routes to embed NPs within hydrogels;[30–34] here, radical polymerization of a monomer–AuNP mixture is carried out in water between two glass slides with defined spacing (details are found in the Experimental Section). Small (millimeter scale) squares are punched from the polymerized NC gel sheets and submersed in a phosphate buffer solution (pH 7.3, 0.1 M NaCl) and illuminated with patterns of white light generated using a digital micro-mirror array, projected through an inverted microscope objective lens.

Figure 1 B shows selected fully reversible shape transformations of a single 25 μm thick NC gel sheet in aqueous solution at 30 °C (see also movie SV1 in the Supporting Information). Regions illuminated with white light contract in volume, yielding steady-state buckled shapes that can be qualitatively understood from prior studies on sheets with pre-patterned deformation.[6,7,15,35–37] A single rectangular stripe drives rolling into an axisymmetric "bottle-like" shape (ii), stripes oriented at an angle to the sheet edges yields a helical roll (iii), illuminating the edges of the sheet

[*] A. W. Hauser, J.-H. Na, R. C. Hayward
Department of Polymer Science & Engineering
University of Massachusetts, Amherst, MA 01003 (USA)
E-mail: hayward@umass.edu
A. A. Evans
Department of Physics, University of Massachusetts
Amherst, MA 01003 (USA)

[**] This work was primarily funded by the US Army Research Office through grant number W911NF-11-1-0080, with additional support for AAE from the US National Science Foundation through grant number DMR-0846582 to C.D. Santangelo.

Supporting information for this article is available on the WWW under http://dx.doi.org/10.1002/anie.201412160.

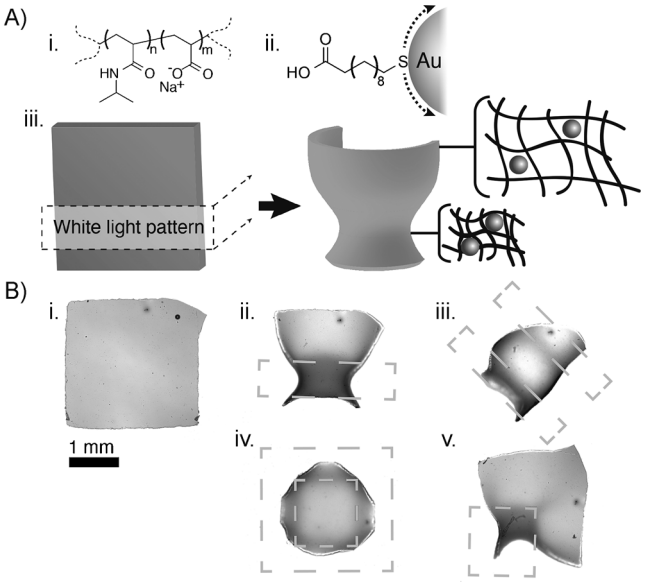

Figure 1. A) Schematic illustration and structures of photothermally reprogrammable gels. B) A single gel sheet is transformed from the flat state (i) subsequently into four selected shapes (ii–v) defined by illumination with white light inside of the dotted boxes (iv: illuminated region is between the two squares).

yields a dome-like elliptic surface (iv), and illuminating one corner yields a wrinkled hyperbolic surface (v).

To better understand this light-induced deformation, we measure the linear swelling ratio (diameter d normalized by its initial value $d_0 = 0.5$ mm) of 100 μm-thick NC gel disks subjected to either flood illumination or global temperature changes (Figure 2). As expected, the gel shrinks in response to increases in both light intensity and temperature, and using the swelling ratio to map between the two curves yields a characteristic local temperature increase provided by a given intensity (Figure 2, inset; $\Delta T = 0$ °C corresponds to 22 °C). Notably, ΔT increases nearly linearly with intensity until ΔT about 8 °C, at which point a break in the curve is seen,

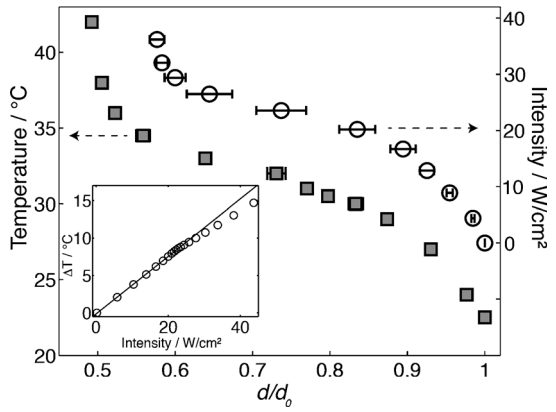

Figure 2. Temperature and intensity as a function of swelling ratio, d/d_0, where d_0 is the diameter at 22 °C without illumination. The inset shows the characteristic photothermal temperature increase as a function of intensity; the solid line shows a fit to the data at low intensities.

perhaps associated with the onset of convection (experimentally observed above ΔT of about 5 °C) or the approach to the limiting deswelling ratio of $d/d_0 \approx 0.5$. Based on these data, patterning experiments are carried out at 30 °C with a light intensity of 5 W cm^{-2} ($\Delta T \approx 2$ °C), which allows for substantial changes in size with minimal convection, and which represents a typical level for light driven deformation of soft polymer actuators.[26,27,38]

We next characterize the swelling kinetics using four gels with initial thicknesses h_0 from 25–100 μm, where the concentration of AuNPs is adjusted to maintain equivalent absorbance of 0.15 (see the Supporting Information). Each gel is first allowed to fully deswell under flood illumination at 22 °C, and subsequently reswelled by turning the light off (Figure 3). All data sets are well-described by single exponential curves, with time constants (Figure 3B, inset) that show a thickness dependence consistent with a poroelastic mass-transport limit, that is, $\tau \approx h_0^2$.[39,40] For sufficiently thin gels, this provides an important advantage over photochemical routes, in that the kinetics of swelling and deswelling can be finely tuned to desired speeds simply by altering the thickness or porosity of the gel. Here, we find characteristic

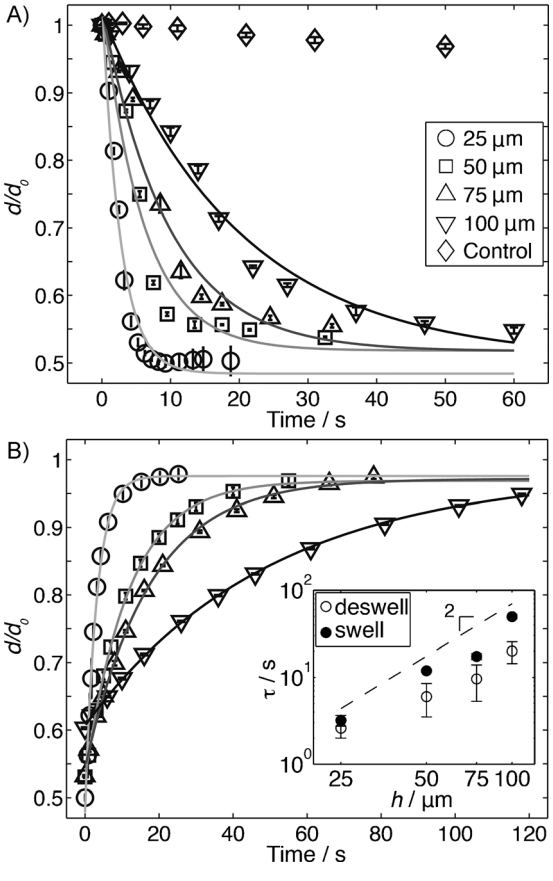

Figure 3. A) Deswelling kinetics under flood illumination at 22 °C for gels with the indicated initial thicknesses (a control sample lacking AuNPs is shown for comparison), and B) subsequent re-swelling after the light is turned off. The inset shows a log–log plot of time constants (single exponential fits shown as solid lines in both A and B) versus thickness.

response times of $\tau \approx 2$–3 s for $h_0 = 25$ μm, while further increases in speed should be easily attainable using thinner gels.

To exercise fine control over the photothermally driven shape transformations of the NC gel sheets, we consider the steady-state temperature profiles generated under illumination. Neglecting convection, the temperature will be governed by Poisson's equation [Eq. (1)],

$$\nabla^2 T = -q(\mathbf{r})/k, \quad (1)$$

where we treat the thermal conductivity k of the NC gel and water as equal. The volumetric heat generation rate q, is proportional to the product of the light intensity, and the absorbance by the gel at position $\mathbf{r}$ (where we ignore the gradient of light intensity through the thickness, appropriate for absorbance values well below 1). Thus, for any arbitrary pattern of light and configuration of the gel sheet, it is possible to solve for the resulting temperature profile using a Green's Function method (see the Supporting Information), and hence to predict the spatial variation in swelling of the gel.

To provide a simple validation of this approach, we expose a square gel sheet to illumination within a rectangle of varying length l, causing the sheets to take on a rolled conformation, with greater curvature for larger l. The steady-state grayscale intensity profiles along the midline are compared to the analytically calculated temperature profiles for a non-deformable sheet, mid-way through the gel thickness along the corresponding line (Figure 4 A). The measured lengths of the deswelled regions (characterized by the full-width at half-maximum; FWHM) are similar to, but slightly smaller than the expected temperature profiles (Figure 4 A,vi), although quantitative agreement between these values is not expected due to the nonlinear relationship between temperature and grayscale value, as well as the reduction in the width of the region of heat generation caused by buckling. In addition to constant intensity illumination, smooth gradients of swelling with desired forms can be generated using halftoned patterns of illumination. For example, Figure 4 B shows the configurations resulting from cubic, quadratic, and linear gradients of light with equal integrated intensities (and thus heat generation). The deformation clearly becomes less localized as the projected intensity is distributed more broadly in space. Thus, while broadening of the projected patterns by thermal diffusion is intrinsic to this approach, by accounting for this broadening, the ultimate shapes of the gel sheets can be fine-tuned in a straightforward manner. More extensive deswelling, and therefore more pronounced out-of-plane buckling can be achieved by reducing the crosslink density of the gel (see movie SV2). In this case, however, the deformation of the sheet can show a more complex time evolution, for example, as buckling causes initially swelled portions of the sheet to fold over into the illuminated region and therefore shrink. It is clear that obtaining quantitative control of the full evolution of gel shape over time will require warping of the pattern of light as the gel deforms, ideally with models that couple heat transfer with an appropriate poroelastic constitutive equation for the gel, and also consider factors such as the change in AuNP concentration with swelling, and the non-zero absorbance of light by the gel film.

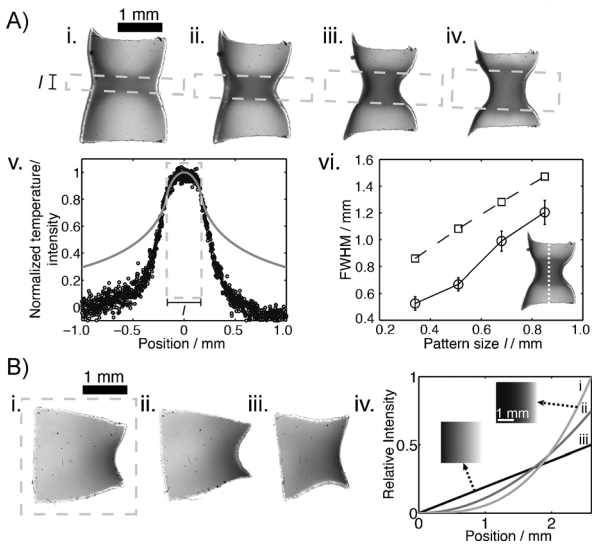

Figure 4. Fine tuning shape transformations of a single gel sheet. A) A light strip of increasing length l, indicated by gray dotted lines, gives rise to increasing curvature of a 25 μm thick sheet. The calculated temperature profile (solid) and experimental intensity data (dots) are shown in (v.) with a dashed box indicating pattern size corresponding to image i. The lengths of the calculated temperature (dashed) and experimental grayscale profiles (solid) are compared in (vi.).
B) Smooth gradients in swelling with different functional forms are provided by halftoned patterns projected onto a sheet of 50 μm in thickness.

Finally, we demonstrate directed motion by repeatedly sweeping a strip of light across a gel sheet (as seen in movie SV3). Interestingly, we find net motion in the direction of the sweep, whereas the simulations of Kuksenok and Balazs for photochemically patterned deformation showed motion in the reverse direction.[15] We speculate that perhaps the presence of time-varying temperature gradients are responsible for the opposite direction observed here, as Kuksenok and Balazs also found motion towards higher temperature regions when an orthogonal temperature gradient was applied during sweeping with light. While fully understanding this difference requires further study, the ability to direct the motion of such gels in addition to dynamically reconfiguring their shapes opens the door to highly adaptable elastic sheets.

In summary, we have developed a method to dynamically transform and reconfigure 2D hydrogel sheets into predictable and complex 3D shapes not limited by pre-programmed patterns within the material. Using the SPR absorption of dispersed AuNPs and patterned illumination with visible light, rapid and localized photothermal deformation occurs in illuminated regions due to steady-state temperature gradients that can be understood by classical heat conduction equations. An almost limitless number of 3D shapes can easily be achieved from a single sheet, paving the way for continuously reconfigurable materials for soft robotics, drug delivery systems, and microfluidic devices.

Experimental Section

Nanoparticle synthesis: The synthesis of AuNPs has been described in detail elsewhere.[41] Briefly, to an aqua regia cleaned vial and stir bar, 0.0495 g (1 equiv) of $AuPPh_3Cl$ was dissolved in 10 mL of 1:1 ethanol:chloroform. Then, 0.0366 g (2 equiv) of mercaptoundecanoic acid (Aldrich, $\geq 99\,\%$) was added to the vial, followed by heating (using a preheated 55 °C oil bath), and finally, 0.087 g (10 equiv) of *tert*-butylamine borane (Aldrich, 97 %) was added in one portion. The solution quickly turns from colorless to brown to light red-purple, and then darkens over the course of 2 h. The AuNPs were purified by three precipitation-centrifugation cycles: the solution was precipitated with 30 mL of THF, centrifuged (7800 RPM, 10 min), and redissolved in 1 mL of methanol.

Gel preparation: To a Teflon lined vial containing 0.5 mg of dried AuNPs, 148 μL of a 0.24 $g\,mL^{-1}$ aqueous solution of *N*-isopropylacrylamide (Tokyo Chemical Industry, > 98 %), 30.5 μL of a 0.1 $g\,mL^{-1}$ aqueous solution of sodium acrylate, 19.4 μL of a 0.02 $g\,mL^{-1}$ aqueous solution of methylene bisacrylamide and 2.1 μL of deionized water, were added sequentially. The solution was degassed, and 1 μL of *N*,*N*,*N*′,*N*′-tetramethylethylenediamine (Aldrich, $\geq 99\,\%$) and 2 μL of ammonium persulfate solution (0.1 $g\,mL^{-1}$, Aldrich, $\geq 98\,\%$) were added to initiate polymerization. This pre-gel mixture was injected between two glass slides spaced by 100 μm Kapton spacers, placed in a vessel, purged with nitrogen and allowed to polymerize for 1 h or longer. Gels were placed in buffer solution and allowed to sit for 15 h or longer, and then washed by two additional fresh buffer solution transfers. Sodium acrylate was included as a comonomer to allow the swelling ratio and response to be adjusted with salt. Squares and circles were manually punched from the gel sheets. Gels with thicknesses of 25, 50 and 75 μm were prepared using identical procedures, except with respective AuNP contents of 2, 1, and 0.67 mg.

Microscope set-up: All experiments were conducted using a Nikon Eclipse Ti inverted microscope with a Lumencore Spectra LED light source reflected off a Texas Instruments DLP Discovery 4100 digital micro-mirror array before reaching the objectives (4×, NA = 0.2 and 10×, NA = 0.5; NA = numerical aperture).

Image analysis: Grayscale profiles were found with ImageJ image analysis software by taking the gray values along the central line (inset: Figure 4 Avi), normalizing between 0 and 1, then taking the FWHM. Temperature profiles were plotted from Equation (S5) using length, width, and height values of the undeformed gel.

Keywords: gold nanoparticles · hydrogels · nanocomposites · photothermal deswelling · soft matter

How to cite: *Angew. Chem. Int. Ed.* **2015**, *54*, 5434–5437
Angew. Chem. **2015**, *127*, 5524–5527

[1] L. Ionov, *Langmuir* **2014**, DOI: 10.1021/la503407z.
[2] E. Sharon, E. Efrati, *Soft Matter* **2010**, *6*, 5693–5704.
[3] D. Chen, J. Yoon, D. Chandra, A. J. Crosby, R. C. Hayward, *J. Polym. Sci. Part B* **2014**, *52*, 1441–1461.
[4] D. H. Gracias, *Curr. Opin. Chem. Eng.* **2013**, *2*, 112–119.
[5] J. Kim, J. A. Hanna, M. Byun, C. D. Santangelo, R. C. Hayward, *Science* **2012**, *335*, 1201–1205.
[6] J. Kim, J. A. Hanna, R. C. Hayward, C. D. Santangelo, *Soft Matter* **2012**, *8*, 2375–2381.
[7] Y. Klein, E. Efrati, E. Sharon, *Science* **2007**, *315*, 1116–1120.
[8] Z. L. Wu, M. Moshe, J. Greener, H. Therien-Aubin, Z. Nie, E. Sharon, E. Kumacheva, *Nat. Commun.* **2013**, *4*, 1586.
[9] L. T. de Haan, C. Sánchez-Somolinos, C. M. W. Bastiaansen, A. P. H. J. Schenning, D. J. Broer, *Angew. Chem. Int. Ed.* **2012**, *51*, 12469–12472; *Angew. Chem.* **2012**, *124*, 12637–12640.
[10] K. M. Lee, T. J. Bunning, T. J. White, *Adv. Mater.* **2012**, *24*, 2839–2843.
[11] H. Thérien-Aubin, Z. L. Wu, Z. Nie, E. Kumacheva, *J. Am. Chem. Soc.* **2013**, *135*, 4834–4839.
[12] C. Yu, Z. Duan, P. Yuan, Y. Li, Y. Su, X. Zhang, Y. Pan, L. L. Dai, R. G. Nuzzo, Y. Huang, et al., *Adv. Mater.* **2013**, *25*, 1541–1546.
[13] E. Palleau, D. Morales, M. D. Dickey, O. D. Velev, *Nat. Commun.* **2013**, *4*, 2257.
[14] R. R. Kohlmeyer, P. R. Buskohl, J. R. Deneault, M. F. Durstock, R. A. Vaia, J. Chen, *Adv. Mater.* **2014**, *26*, 1–6.
[15] O. Kuksenok, A. C. Balazs, *Adv. Funct. Mater.* **2013**, *23*, 4601–4610.
[16] C. J. Barrett, J. Mamiya, K. G. Yager, T. Ikeda, *Soft Matter* **2007**, *3*, 1249–1261.
[17] K. Matsubara, M. Watanabe, Y. Takeoka, *Angew. Chem. Int. Ed.* **2007**, *46*, 1688–1692; *Angew. Chem.* **2007**, *119*, 1718–1722.
[18] J. Wei, Y. Yu, *Soft Matter* **2012**, *8*, 8050–8059.
[19] B. Ziółkowski, L. Florea, J. Theobald, F. Benito-Lopez, D. Diamond, *Soft Matter* **2013**, *9*, 8754–8760.
[20] T. Satoh, K. Sumaru, T. Takagi, T. Kanamori, *Soft Matter* **2011**, *7*, 8030–8034.
[21] S. R. Sershen, G. A. Mensing, M. Ng, N. J. Halas, D. J. Beebe, J. L. West, *Adv. Mater.* **2005**, *17*, 1366–1368.
[22] A. Suzuki, T. Tanaka, *Nature* **1990**, *346*, 345–347.
[23] D. Kim, H. S. Lee, J. Yoon, *RSC Adv.* **2014**, *4*, 25379–25383.
[24] E. Wang, M. S. Desai, S.-W. Lee, *Nano Lett.* **2013**, *13*, 2826–2830.
[25] J. Yoon, P. Bian, J. Kim, T. J. McCarthy, R. C. Hayward, *Angew. Chem. Int. Ed.* **2012**, *51*, 7146–7149; *Angew. Chem.* **2012**, *124*, 7258–7261.
[26] A. Barhoumi, W. Wang, D. Zurakowski, R. S. Langer, D. S. Kohane, *Nano Lett.* **2014**, *14*, 3697–3701.
[27] Z. Zhu, E. Senses, P. Akcora, S. A. Sukhishvili, *ACS Nano* **2012**, *6*, 3152–3162.
[28] A. O. Govorov, W. Zhang, T. Skeini, H. Richardson, J. Lee, N. A. Kotov, *Nanoscale Res. Lett.* **2006**, *1*, 84–90.
[29] S. Eustis, M. A. El-Sayed, *Chem. Soc. Rev.* **2006**, *35*, 209–217.
[30] C. Wang, N. T. Flynn, R. Langer, *Adv. Mater.* **2004**, *16*, 1074–1079.
[31] V. Pardo-Yissar, R. Gabai, A. N. Shipway, T. Bourenko, I. Willner, *Adv. Mater.* **2001**, *13*, 1320–1323.
[32] S. R. Sershen, S. L. Westcott, N. J. Halas, J. L. West, *J. Biomed. Mater. Res.* **2000**, *51*, 293–298.
[33] X. Zhao, X. Ding, Z. Deng, Z. Zheng, Y. Peng, C. Tian, X. Long, *New J. Chem.* **2006**, *30*, 915–920.
[34] E. Marsich, A. Travan, I. Donati, A. Di Luca, M. Benincasa, M. Crosera, S. Paoletti, *Colloids Surf. B* **2011**, *83*, 331–339.
[35] M. Byun, C. D. Santangelo, R. C. Hayward, *Soft Matter* **2013**, *9*, 8264–8273.
[36] E. Efrati, E. Sharon, R. Kupferman, *J. Mech. Phys. Solids* **2009**, *57*, 762–775.
[37] M. A. Dias, J. A. Hanna, C. D. Santangelo, *Phys. Rev. E* **2011**, *84*, 036603.
[38] M. Camacho-Lopez, H. Finkelmann, P. Palffy-Muhoray, M. Shelley, *Nat. Mater.* **2004**, *3*, 307–310.
[39] C.-Y. Hui, V. Muralidharan, *J. Chem. Phys.* **2005**, *123*, 154905–154912.
[40] J. Yoon, S. Cai, Z. Suo, R. C. Hayward, *Soft Matter* **2010**, *6*, 6004–6012.
[41] N. Zheng, J. Fan, G. D. Stucky, *J. Am. Chem. Soc.* **2006**, *128*, 6550–6551.

Received: December 18, 2014
Revised: February 18, 2015
Published online: March 5, 2015

